Hindawi
Wireless Communications and Mobile Computing
Volume 2022, Article ID 8494630, 13 pages
https://doi.org/10.1155/2022/8494630

*Research Article*

# Reconfigurable Intelligent Surface Assisted Non-Terrestrial NOMA Networks

**Xuanhao Lian**,[1] **Xinwei Yue**,[1] **Xuehua Li**,[1] **Xiang Yun**,[2] **Tian Li**,[3] **and Dehan Wan**[4]

[1]*Key Laboratory of Information and Communication Systems, Ministry of Information Industry and Also with the Key Laboratory of Modern Measurement & Control Technology, Ministry of Education, Beijing Information Science and Technology University, Beijing 100101, China*
[2]*Baicells Technologies co. Ltd, Beijing 100095, China*
[3]*The 54th Research Institute of China Electronics Technology Group Corporation, Shijiazhuang Hebei 050081, China*
[4]*Guangdong University of Finance, Guangzhou 510521, China*

Correspondence should be addressed to Xuehua Li; lixuehua@bistu.edu.cn

Received 30 June 2022; Revised 27 August 2022; Accepted 31 August 2022; Published 19 September 2022

Academic Editor: Jun Li



This paper considers the application of reconfigurable intelligent surface (RIS) to non-terrestrial non-orthogonal multiple access (NOMA) networks. More specifically, the performance of a pair of non-orthogonal users for RIS assisted non-terrestrial NOMA networks is investigated over large-scale fading and Nakagami-$m$ fading cascaded channel. The exact and asymptotic expressions of outage probability are derived for the nearby user and distant user with the imperfect successive interference cancellation (SIC) and perfect SIC schemes. Based on the approximated results, the diversity orders of these two users are obtained in the high signal-to-noise ratios. The simulation results are used to verify the theoretical derivations and find that: 1) The outage behaviors of RIS assisted non-terrestrial NOMA networks outperforms than that of orthogonal multiple access; 2) By increasing the number of reflecting elements of RIS and Nagakami-$m$ fading factors $m'$ and $\Omega$, RIS-assisted non-terrestrial NOMA networks are able to achieve the enhanced outage performance.

## 1. Introduction

With the development of the fifth-generation (5G) communication technologies, mobile communication has gradually entered the era of high-speed interconnections [1], and research on the sixth-generation (6G) communication technologies has gradually been carried out to aim at the achievement of global coverage, enhanced spectrum efficiency, better security and higher intelligence level [2]. As one of the key technologies of 6G, non-orthogonal multiple access (NOMA) has ability to support multiple users' information which is linearly superposed at the same physical resource over different power levels. The authors of [3] well explained the development status and working principle of NOMA. And in existing researches, NOMA technologies have been applied in the Internet of Things industry for improving the spectral efficiency to make up for the shortage of spectrum resources [4]. Also NOMA can not only meet the requirements of communication transmission, but also have more prominent advantages in energy consumption [5].

Recent years have witnessed a spurt of progress in NOMA technologies and studies about terrestrial scenarios have provided new insights into NOMA application. The specific concept of NOMA is that multiple users' signals are overlaid at the transmitting end by employing the superposition coding scheme. At receiving end, the successive interference cancellation (SIC) is carried out to peel off the desired signal [6]. In the SIC process, the strong users firstly decode all weak users'signals and remove them for the preparation to decode their own signals. The weak users directly decode their own signals by treating the signals of all strong users as interference. It has shown that NOMA is capable of providing the enhanced system efficiency and user fairness

with respect to orthogonal multiple access (OMA), and the authors of [7] provided a systematic treatment of NOMA from its combination with multiple-input multiple-output technologies to cooperative NOMA. The performance of unified NOMA framework was surveyed in terms of outage probability by taking into account both perfect SIC (pSIC) and imperfect SIC (ipSIC) [8]. Furthermore, the ideology of NOMA was extended to cooperative communications [9], where the nearby user with better channel conditions was reviewed as the relaying to forward information for distant user. In [10], the authors analyzed the ergodic rate of decode-and-forward (DF) relaying based cooperative NOMA systems. With the emphasis on physical layer communications, the authors of [11] investigated the secrecy outage behaviors of NOMA networks with the aid of stochastic geometry. Additionally, the authors in [12] proposed a backscatter assisted NOMA network and confirmed that the transmission reliability and effectiveness can be enhanced without impairing the spectrum efficiency. Applying NOMA to random access, the NOMA assisted semi-grand free transmission was proposed in [13], which solves the problems of no upper limit on the number of admitted users. A channel differences exploiting scheme for NOMA was discussed in [14], where a dual-hop cooperative relaying network was proposed and a best relay was picked up as an active node for transmission. For better reliability of NOMA based networks, the authors of [15] suggested a multi-band scheduling policy which accommodates the near and far users through sub-band exploring.

Non-terrestrial communication network is one of the important application scenarios for 6G networks and a lot of attention have been received on it [16]. The NOMA technology can also be incorporated into the space-air-ground networks and play a pivotal role in the non-terrestrial communication scenarios [17]. Cooperative NOMA communication protocol was applied to a satellite-terrestrial networks in [18], in which outage performance was notably improved because of the application of NOMA scheme. An unmanned aerial vehicle (UAV) was used as a relay in [19], where NOMA scheme was utilized to transmit signals to solve the detection-vector optimization problem about UAV signal collection. Additionally for NOMA-UAV networks in [20], a path following algorithm was proposed to formulate the max-min rate optimization under NOMA scheme with a UAV serving a large number of ground users. Multi-layer NOMA satellite network was studied in [21], joint user pairing and power allocation scheme were introduced to deal the frequency interference coordination between different orbits. Different from studying on geostationary orbit scenarios, the authors of [22] studied a low earth orbit satellite NOMA system, huge time delay and Doppler shift were taken into consideration carefully. In terms of performance analysis, the authors in [23] analyzed the outage behaviors of satellite NOMA networks based on Shadowed-Rician fading channels, the diversity order of the users have achieved with ipSIC and pSIC scheme, respectively. With the perspective on decoding and transmitting mode in [24], the outage performance for amplify-and-forward (AF) relaying transmission protocols under the hybrid satellite-terrestrial overlay NOMA network was analyzed in detail. Meanwhile in [25], a two-user NOMA-based hybrid satellite-terrestrial relay network was investigated, where the secondary user acquire its desired signal through a DF relay.

Reconfigurable intelligent surface (RIS), as a new type of transmission relay, has ability to correct the wireless channel through a highly controllable software, which paves the way for an intelligent and programmable wireless environment [26–28]. Because of its novelty and greater gain, the RIS-assisted NOMA networks have attracted a large part of research effort [29–31]. In [29], the performance of theoretical framework for the RIS and AF relaying were compared and results showed that RIS-assisted wireless systems outperform the corresponding AF-relaying ones. Further considered in [30], a RIS-aided NOMA network with stochastic geometry model was discussed and the SIC order is proofed to be altered since RISs were able to change the channel quality of users. Multiple RISs assisted NOMA networks was investigated in [31], two scenarios were taken into consideration on whether or not there was a direct link between base station and each user. Additionally discussed in [32], outage performance of RIS-assisted NOMA systems was analyzed with the help of 1-bit coding, in which the performance analysis of cascaded channel condition has been taken into consideration. Moreover in [33], a RIS-assisted NOMA scheme was proposed to demonstrate that more users can be served on each orthogonal spatial direction with the help of RIS. Eventually, as the latest research direction, the authors of [34] have proposed a simultaneously transmitting and reflecting RIS aided NOMA systems, which shared new ideas for RIS deployment in multiple scenarios. For the perspective of grant-free massive access, the authors of [35] have proposed a design to leverage the RIS to for grant-free massive access at millimeter-wave frequency to boost the reliability of communication systems. To solve the°multiplicative fading effect introduced by passive RIS, active RIS [36] has been proposed to compensate for it by reflecting and amplifying the signals, more research on active RIS is also underway. In non-terrestrial networks, the use of RIS technology can make signal transmission more flexible to make up for the problem of satellite communication encountering blind spots. At the same time, the use of RIS technology also provides an idea for the modeling and calculation of cascaded channels, which is worth more in the future research.

*1.1. Motivations and Related Works.* Based on the above-mentioned papers, it lays a solid foundation for NOMA and RIS technologies, the research for integrating the two promising technologies in non-terrestrial networks still gets a lot of upside. RIS can effectively change the transmission mode of electromagnetic waves, including direction, phase and polarization mode, etc. Therefore, introducing RIS into the non-terrestrial communication system to change the phase shifts of the satellite signal and propagate it to the ground users has attracted our attention. It should be noticed that compared with the RIS-assisted terrestrial networks, the RIS-assisted non-terrestrial network has a longer transmission distance and the channel fading needs

reconsideration to fit the scenario. Path Loss gets complicated and channel model needs to be considered for long-distance transmission. Simulation analysis of the transmission power also requires differential modeling. Recently, investigators have examined the effects of RIS communications. To broaden the application of channel mathematical calculation, the probability distribution expression for Rayleigh/Nakagami-$m$ composite fading were deduced in [37], which provides a mathematical method for the computation of cascaded channel models. Simultaneously, the authors of [38] proposed a coherent phase shifting method to deal with the phase shift matrix of RIS, which paves way for the RIS simulation calculation. Using the mathematical models built on the basis of these researches, we aspire to establish a RIS-assisted non-terrestrial NOMA networks with channel model of large-scale fading and Nakagami-$m$ fading cascaded channels, which has not been studied before to the best of our knowledge. More specifically, a pair of users, the nearby user $n$ and distant user $m$, are set to be investigated according to outage probability. The non-terrestrial network communication model based on the transmission of RIS and the channel calculation method under the large-scale fading and Nakagami-$m$ fading cascaded channel model have become the innovations of this paper. Additionally, OMA condition are set to be benchmark and also evaluated seriously. In terms of the above details, the main related work in the paper is described as follows:

(1) We investigate the performance of RIS-assisted non-terrestrial NOMA networks over large-scale fading and Nakagami-$m$ fading cascaded channels. Specifically, cascaded channels are applied in the networks, large-scale fading and Nakagami-$m$ fading distribution for the channel molding are taken into account. The approximated scheme of a Laguerre expansion is applied for the cascaded channel modeling and approximate expression of the cascaded channel is analyzed in detail

(2) We derive the approximate and asymptotic expressions of outage probability for the nearby user $n$ with ipSIC/pSIC and distant user $m$. To get more insights, the diversity orders of the nearby user $n$ with ipSIC/pSIC and distant user $m$ are obtained on the basis of the approximated outage probability expressions. We observe that the diversity orders of user $n$ with ipSIC and user $m$ are related to the configure elements, user order, Rayleigh and Nakagami-$m$ factors

(3) We analyze the outage behaviors of the two users for OMA. It can be further confirmed that outage behaviors of NOMA with pSIC outperforms than that of OMA. Detailed comparisons about the impact of changes in individual variables on outage performance are analyzed as well. The simulation results illustrate that when the configure elements $K$, Nakagami-$m$ shaping parameter $m'$ and scale parameter $\Omega$ increase, the outage performance of the networks turns to be enhanced

*1.2. Organizations and Notations.* The remainder of this paper is structured as follows. System model of the RIS-assisted non-terrestrial NOMA networks is depicted in Section II. In Section III, outage behaviors of the networks is analyzed and expressions of outage probability for the two non-orthogonal users are derived meticulously. In Section IV, simulation results and detailed analysis are presented to consolidate the conclusions obtained in the above sections, while summarized records in Section V.

Notations in this paper describes mainly as follows: $f_X(\cdot)$ and $F_X(\cdot)$ are denote the the probability density function (PDF) and the cumulative distribution function (CDF) of a random variable $X$; $\mathbb{E}[\cdot]$ denotes the expectation operator; $\propto$ denotes "be proportional to".

## 2. System Model

In this paper, we consider a RIS-assisted non-terrestrial NOMA network with a pair of non-orthogonal users among multiple users as shown in Figure 1 and two user equipments (UEs), nearby user $n$ and distant user $m$, are denoted by $D_n$ and $D_m$, respectively. Moreover, taking into account the large transmission distance in the non-terrestrial communication model, the signal of direct connection between each UE and the satellite is strongly attenuated, so we assume that the UEs only communicate with the satellite through the RIS. In order to get the succinct analysis, we only consider that each user is equipped with a single antenna. As a novel type of relay for transmitting signals, the RIS has K discrete reconfigurable elements, each element is controlled by the software systems to affect the phase shifting of signal reflecting, and the reflection-coefficient matrix can be denoted as $\Theta = \text{diag}\,(\beta e^{j\theta_1}, \beta e^{j\theta_2}, \cdots, \beta e^{j\theta_K})$, where $\beta \in [0, 1]$ and $\theta_K \in [0, 2\pi)$ are the amplitude-reflection coefficient and the phase shift variable of $k$-th element of RIS, respectively. Same as above, the reflection-coefficient matrix can be intelligently adjusted for a better way on transmission. The complex channel coefficient between the satellite and RIS is denoted by $\mathrm{h} \in C^{1\times K}$, and the complex channel coefficients between the RIS and $p$-th UE are denoted by $\mathrm{g}_p \in \mathbb{C}^{1\times K}$, where $p \in \{m, n\}$. Specifically, $\mathrm{h} = [h_1, h_2, \cdots, h_K]$, $\mathrm{g}_p = [g_1^p, g_2^p, \cdots, g_K^p]$, and the channels between each element and the satellite can be denoted by [39] $h_k = \rho\sqrt{G_t}\sqrt{\lambda/(4\pi d)^2}\sqrt{G_i}$, where $\rho \sim CN(0, 1)$ represents the small-scale fading, $G_t$ and $G_i$ are lobe gains of antennas at satellite end and users end, respectively. $\sqrt{\lambda/(4\pi d)^2}$ is the free space path loss, $\lambda$ and $d$ are the wave length and the distance between the satellite and RIS, respectively. In order to facilitate subsequent calculations, we denote $\bar{\lambda} = \sqrt{G_i}\sqrt{\lambda/(4\pi d)^2}\sqrt{G_t}$. Without loss of precision, in order to visually represent the performance of users' channel under different transmission distances, the ordered cascaded channel gains has been taken into account, so we consider $|h\Theta \mathrm{g}_m^T|^2 \le |h\Theta \mathrm{g}_n^T|^2$. It is worth noting that the ordering of channels also determines the order of nearby and distant users.

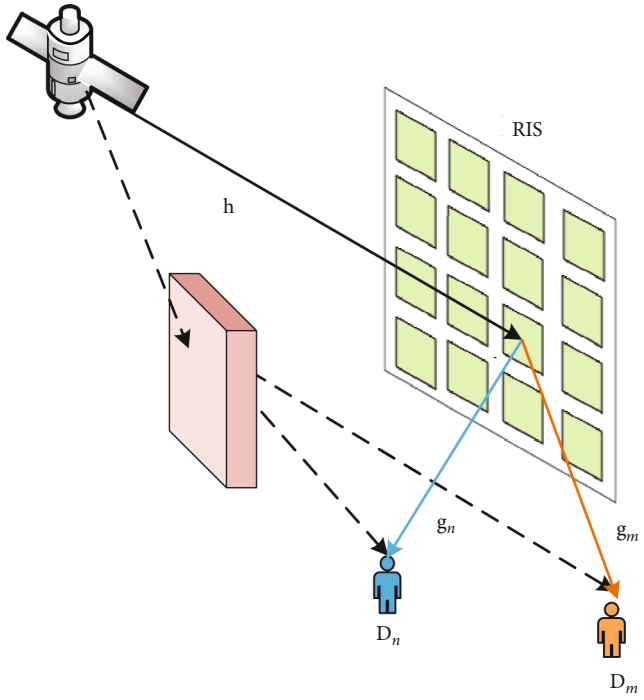


FIGURE 1: System model of RIS-assisted non-terrestrial NOMA networks.

*2.1. Signal Model.* The superposed signals are broadcast to the two UEs by reflection of the RIS, and the received signal $y_p$ at the $p$-th UE reflected by RIS is given by

$$y_p = h\Theta \mathbf{g}_p^T \left( \sqrt{a_n P} x_n + \sqrt{a_m P} x_m \right) + n_p, \tag{1}$$

where $P$ is the transmit power, $x_n$ and $x_m$ are the transmitted normalized power signal at $D_n$ and $D_m$. For elaboration, $\mathbb{E}\{x_n^2\} = \mathbb{E}\{x_m^2\} = 1$. $a_n$ and $a_m$ are power allocation coefficients, $a_n \le a_m$ with $a_n + a_m = 1$,which is for the user's fairness of the NOMA transmission. Meanwhile, $n_p$ is the additive white Gaussian noise (AWGN) at $D_p$

In NOMA communication protocols, the transmitting end use the non-orthogonal transmission scheme to allocate users' transmission power. At the receiving end, the SIC receiver decode the signal for each of the users' part, and the process of SIC is the user signal with weaker power allocation regards the user signal with stronger power as interference and decodes its own signal, while the user signal with stronger power allocation needs to decode and subtract the user signal with weaker power allocation first, and then decode its own signal. Based on the basic principles of NOMA, the received signal-to-interference-plus-noise ratio (SINR) at $D_n$ to detected $D_m$'s information $x_m$ is given by

$$\gamma_{D_n \longrightarrow D_m} = \frac{\rho \left| \mathbf{h}\Theta \mathbf{g}_n^T \right|^2 a_m}{\rho \left| \mathbf{h}\Theta \mathbf{g}_n^T \right|^2 a_n + 1}, \tag{2}$$

where $\rho = P/N_0$ denotes the transmit signal-to-noise ratio (SNR).

After SIC process, the received signal at $D_n$ to detect its own information $x_n$ is given by

$$\gamma_{D_n} = \frac{\rho \left| \mathbf{h}\Theta \mathbf{g}_n^T \right|^2 a_n}{\varpi \rho |h_I|^2 + 1}, \tag{3}$$

where $\varpi \in \{0, 1\}$, $\varpi = 0$ and $\varpi = 1$ denotes the pSIC and ipSIC operation, respectively. Without loss of generality, $h_I \sim CN(0, \Omega_I)$ is the corresponding complex channel coefficient of the residual interference form ipSIC [40, 41], which is modeled as the Rayleigh fading.

When the receiver at $D_m$ get the superposed signal, the decoding process is to treat the signal of $D_n$ part as interference, and treat the signal of $D_m$ part as desired signal. Therefore, the received SINR at $D_m$ to detected its own information $x_m$ by treating the signal $x_n$ as interference is given by

$$\gamma_{D_m} = \frac{\rho \left| \mathbf{h}\Theta \mathbf{g}_m^T \right|^2 a_m}{\rho \left| \mathbf{h}\Theta \mathbf{g}_m^T \right|^2 a_n + 1}. \tag{4}$$

For the baseline of OMA scheme, which is chosen for the purpose of comparing to the NOMA scheme, the SNR of the $p$-th user under the OMA scheme can be given by

$$\gamma_p^{OMA} = \rho \left| h\Theta \mathbf{g}_p^T \right|^2. \tag{5}$$

*2.2. Channel Model.* In non-terrestrial communication systems, there is an extreme long distance from the satellite to the RIS and the signals are mainly attenuated by free-space path loss. Therefore, a free space transmission model is often used to predict the received signals in a line-of-sight environment [42], and the signals should mainly experience large-scale fading [39], so we consider the channels between satellite and RIS are modeled as large-scale fading channels. The channels between RIS and the UEs are mainly None Line of Sight, then we consider the RIS-UEs channels to be modeled as Nakagami-$m$ fading channels. Noted that large-scale fading is a kind of Rayleigh fading, our analysis of large-scale fading is based on the analysis of Rayleigh fading. So we denote that $[h_1, h_2, \cdots, h_K]$ are independent identically distributed (i.i.d.) Rayleigh random variables (RVs), and $[g_1, g_2, \cdots, g_K]$ are i.i.d. Nakagami-$m$ RVs with shape parameter $m'$ and spread parameter $\Omega$, and all of the $h_n$ and $g_n$ are independent, either.

From the perspective of enhancing the network performance, coherent phase shifting design are selected to optimize the phase shifting process for RIS-assisted non-terrestrial NOMA networks. In coherent phase shifting scheme, the phase shift of each reflecting and transmitting element is matched with the phases of its incoming and outgoing fading channels, and coherent phase shifting scheme has better analytical performance than that of the random phase shifting scheme. it can simulate a more idealized and better channel state, and can reflect the system characteristics more intuitively and conveniently. For the coherent

phase shifting scheme [38], we can define $h\Theta g_p^T = \sum_{n=1}^{K} e^{-j\theta_n} h_n g_n$, where $h_n$ and $g_n$ denote the $n$-th element of h and $g_p$, $\theta_n$ denotes the phase shift of the $n$-th reflecting element of the RIS. Match the phase shifts of the RIS and the phases of the RIS fading gains, we can obtain $h\Theta g_p^T = \sum_{n=1}^{K} |h_n g_n|$

To take explicit insights for understanding, we first consider one single cascaded channel from the satellite to the RIS to the UE, then analyze the multiple parallel cascaded channels on the basis of single cascaded channel. The PDF of a single Rayleigh cascade Nakagami-$m$ fading channel can be given by [37].

$$f_{RN}(x) = \frac{4x^{m'}}{\Gamma\left(m'\right)} \left(\frac{m'}{\widehat{r}_1^2 \widehat{r}_2^2}\right)^{\left(1+m'\right)/2} K_{1-m'}\left(2x\sqrt{\frac{m'}{\widehat{r}_1^2 \widehat{r}_2^2}}\right), \quad (6)$$

where $m'$ is the shaping parameter of the Nakagami-$m$ RV, $\widehat{r}_i$ is the root-mean square value of the received signal envelope $R_i$, from [43],

$$\widehat{r}_i \triangleq \sqrt{\mathbb{E}\left[R_i^2\right]} = \frac{\bar{r}_i \Gamma(\mu_i)[(1+\kappa_i)\mu_i]^{1/2}}{\Gamma(\mu_i + 1/2) e^{-\kappa_i \mu_i} {}_1F_1(\mu_i + 1/2\,;\mu_i\,;\kappa_i \mu_i)}, \quad (7)$$

where $i \in \{1, 2\}$, $\mathbb{E}[R_i^2]$ represents the second moment of $R_i$, and $R_i$ is the received signal envelope. $\bar{r}_i = \mathbb{E}[R_i]$. $\Gamma(\cdot)$ is the gamma function ([44], Eq. (8.310.1)), ${}_1F_1(a\,;b\,;z)$ denotes the confluent hypergeometric function ([44], Eq. (9.210.1)). $K_\phi(\cdot)$ is the ¦Õth-order modified Bessel function of the second kind ([44], Eq. (8.432)).

To simplify expression, we denote $\varphi_n = |h_n g_n|$. It can be derived that the mean and variance of $\varphi_n$ are, respectively

$$E(\varphi_n) = \bar{\lambda}\sigma \sqrt{\frac{\pi}{2}} \frac{\Gamma\left(m' + 1/2\right)}{\Gamma\left(m'\right)} \left(\frac{\Omega}{m'}\right)^{1/2}, \quad (8)$$

$$Var(\varphi_n) = \bar{\lambda}^2 \left[2\Omega\sigma^2 - \frac{\pi\Omega\sigma^2}{2m'} \frac{\Gamma^2\left(m' + 1/2\right)}{\Gamma^2\left(m'\right)}\right]. \quad (9)$$

However, the signal is transmitted by the reflecting of $K$ elements of RIS from each reflecting element to each user. Therefore, there is $K$ parallel separate cascaded channels that should be taken into consideration for the signals'transmission.

Let $\varphi = \sum_{n=1}^{K} \varphi_n$ to denote the $K$ parallel cascaded channels. According to ([45], Sec. 2.2.2), the first term of the Laguerre polynomials can be used to approximate the PDF of $\varphi$ and $\varphi^2$, which are, respectively, given by

$$f_\varphi(x) = \frac{x^a}{b^{a+1}\Gamma(a+1)} \exp\left(-\frac{x}{b}\right), \quad (10)$$

$$f_{\varphi^2}(x) = \frac{1}{2\sqrt{x}} \frac{\left(\sqrt{x}\right)^a}{b^{a+1}\Gamma(a+1)} \exp\left(-\frac{\sqrt{x}}{b}\right), \quad (11)$$

, respectively. Where $a = K[E(\varphi_n)]^2 / Var(\varphi_n) - 1$, $b = Var(\varphi_n)/E(\varphi_n)$. Calculated on the basis of (11), and with the definition of the lower incomplete gamma function $\gamma(\alpha, x) = \int_0^x e^{-t} t^{\alpha-1} dt$ ([44], Eq. (8.350.1)), the cumulative distribution function (PDF) of $\varphi^2$ can be given by

$$F_{\varphi^2}(y) = \frac{\gamma\left(a+1, \left(\sqrt{y}/b\right)\right)}{\Gamma(a+1)}. \quad (12)$$

## 3. Outage Probability

Outage probability is an important performance evaluation metric for wireless communication systems. In communications, if the signals' transmission rate is higher than the channel capacity, then the transmitted signal cannot be received completely and correctly. In another word, when the signals' transmission rate is lower than the service reliability transmission rate, the outage occurs. In this section, the outage performance of the RIS-assisted non-terrestrial NOMA networks is analyzed, the outage probability for the nearby user $n$ with ipSIC/pSIC and distant user $m$ are discussed in detail.

*3.1. The Outage Probability of Nearby User n.* According to NOMA protocol, for the nearby user $n$, during the SIC process, the SIC receiver should first detect and decode the signal of the distant user $m$, and then decode its own signal. Therefore, outage occurs when 1) user $n$ cannot detect the signal $x_m$; 2) user $n$ can detect the signal $x_m$ but cannot detect the signal $x_n$. The outage probability of the nearby user $n$ can be written as

$$P_{D_n}^{ipSIC} = \Pr\left(\gamma_{D_n \longrightarrow D_m} < \gamma_{th_m}\right) + \Pr\left(\gamma_{D_n \longrightarrow D_m} > \gamma_{th_m}, \gamma_{D_n} < \gamma_{th_n}\right), \quad (13)$$

where $\gamma_{th_n} = 2^{R_n} - 1$ and $\gamma_{th_m} = 2^{R_m} - 1$ represent the target SNRs of user $n$ and user $m$ for detecting and decoding the signals $x_n$ and $x_m$, with $R_n$ and $R_m$ being the target rate for $D_n$ to detect $x_n$ and $x_m$, respectively. For further explanation, the following theorem illustrates the outage probability of nearby user $n$

**Theorem 1.** *Under large-scale fading and Nakagami-m fading cascaded channels, the approximate expression for outage probability of the nearby user n with ipSIC for RIS-assisted non-terrestrial NOMA networks is given by*

$$P_{D_n}^{ipSIC} \approx S_n \sum_{l=0}^{M-n} \sum_{u=0}^{U} M - n_l \times \frac{(-1)^l A_u}{(n+l)[\Gamma(a+1)]^{n+l}} \left[\gamma\left(a+1, \frac{G_u}{\bar{\lambda} b}\right)\right]^{n+l}, \quad (14)$$

where $\varpi = 1$, $G_u = \sqrt{(\Omega_I \varpi \rho x_u + 1)\theta}$, $S_n = M!/(M-n)!(n-1)!$, $\theta = \gamma_{th_n}/a_n \rho$. With the help of Gauss-Laguerre quadrature, $x_u$ is the abscissas and the $u$-th zero point of Laguerre polynomial $L_u(x_u)$, $A_u$ is the $u$-th weight, and can be denoted by $A_u = [(U+1)!]^2 / x_u [L'_{U+1}(x_u)]^2$, $u = 0, 1, \cdots, U$.

Specifically, $M$ is the total number of users, $n$ is the order of the current user.

*Proof.* By using the definition expression of the outage event of the nearby user $n$ and substituting (2) and (3) into (13), the outage probability of user $n$ with ipSIC can be given by (15) at the top of the next page.

$$P_{D_n}^{ipSIC} = \Pr\left(\frac{\rho\left|\mathbf{h}\Theta\mathbf{g}_n^T\right|^2 a_m}{\rho\left|\mathbf{h}\Theta\mathbf{g}_n^T\right|^2 a_n + 1} < \gamma_{th_m}\right) + \Pr\left(\frac{\rho\left|\mathbf{h}\Theta\mathbf{g}_n^T\right|^2 a_m}{\rho\left|\mathbf{h}\Theta\mathbf{g}_n^T\right|^2 a_n + 1} > \gamma_{th_m}, \frac{\rho\left|\mathbf{h}\Theta\mathbf{g}_n^T\right|^2 a_n}{\varpi\rho|h_I|^2 + 1} < \gamma_{th_n}\right). \tag{15}$$

And do further calculations, it can be derived as follows:

$$\begin{aligned} P_{D_n}^{ipSIC} &= \Pr\left[0 < \left|\mathbf{h}\Theta\mathbf{g}_n^T\right|^2 < \left(\varpi|h_I|^2\rho + 1\right)\theta\right] \\ &= \int_0^{\infty}\int_0^{(x\varpi\rho+1)\theta} f_{|h_{LI}|^2}(x)\widehat{f}_{\varphi^2}(y)dxdy \\ &= \int_0^{\infty} \widehat{F}_{\varphi^2}[(x\varpi\rho + 1)\theta]\frac{1}{\Omega_I}e^{-(x/\Omega_I)}dx, \end{aligned} \tag{16}$$

where $\widehat{F}_{\varphi^2}(\cdot)$ means the CDF of the sorted channel. According to [46], the relationship between the PDFs of the post-sorted and pre-sorted channels can be expressed as follows

$$\widehat{F}_{\varphi^2}(x) = \frac{M!}{(M-p)!(p-1)!}\sum_{l=0}^{M-p} M - p_l \times \frac{(-1)^l}{p+l}\left[F_{\varphi^2}(x)\right]^{p+l}. \tag{17}$$

In this formula, $M$ represents the total number of users, $p$ is the order of the current user. Finally, substituting (12) into (17) and recombining (16), (14) can be derived. The proof is completed. □

**Corollary 2.** *When it comes to the special condition of $\varpi = 0$, the approximate expression for outage probability of the nearby user n with pSIC scheme for RIS-assisted non-terrestrial NOMA networks can be expressed by*

$$P_{D_n}^{pSIC} \approx S_n \sum_{l=0}^{M-n} M - n_l \frac{(-1)^l}{n+l}\left[\frac{\gamma\left(a+1, \left(\sqrt{\theta}/\bar{\lambda}b\right)\right)}{\Gamma(a+1)}\right]^{n+l}. \tag{18}$$

*3.2. The Outage Probability of Distant User m.* For the distant user $m$, it only needs to detect and decode its own signal and treat the signal from the nearby user $n$ as interference. So, when the distant user $m$ cannot detect and decode its own signal, the outage occurs. Therefore, the outage probability of the distant user $m$ can be expressed as

$$P_{D_m} = \Pr\left(\gamma_{D_m} < \gamma_{th_m}\right). \tag{19}$$

**Theorem 3.** *Under large-scale fading and Nakagami-m fading cascaded channels, the approximate expression for outage probability of the distant user m for RIS-assisted non-terrestrial NOMA networks is given by*

$$P_{D_m} \approx S_m \sum_{l=0}^{M-m} M - m_l \frac{(-1)^l}{(n+l)[\Gamma(a+1)]^{m+l}} \times \left[\gamma\left(a+1, \frac{\sqrt{\gamma^*}}{\bar{\lambda}b}\right)\right]^{m+l}, \tag{20}$$

where $S_m = M!/(M-m)!(m-1)!$, $\gamma^* = \gamma_{th_m}/\rho(a_m - \gamma_{th_m} a_n)$

*Proof.* By substituting (4) into (19), the outage probability of $D_n$ can be calculated as

$$\begin{aligned} P_{D_m} &= \Pr\left(\frac{\rho\left|\mathbf{h}\Theta\mathbf{g}_m^T\right|^2 a_m}{\rho\left|\mathbf{h}\Theta\mathbf{g}_m^T\right|^2 a_n + 1} < \gamma_{th_m}\right) \\ &= \Pr\left[\left|\mathbf{h}\Theta\mathbf{g}_m^T\right|^2 < \frac{\gamma_{th_m}}{\rho\left(a_m - \gamma_{th_m} a_n\right)}\right] = \int_0^{\gamma^*} \widehat{f}_{\varphi^2}(y)dy, \end{aligned} \tag{21}$$

where $\widehat{f}_{\varphi^2}(y)$ is the PDF of the sorted channel gain, according to [46], it can be defined as

$$\widehat{f}_{\varphi^2}(x) = \frac{M!}{(M-p)!(p-1)!} f_{\varphi^2}(x) \times \left[F_{\varphi^2}(x)\right]^{p-1}\left[1 - F_{\varphi^2}(x)\right]^{M-p}. \tag{22}$$

Specifically, $\int_0^x \widehat{f}_{\varphi^2}(t)dt = \widehat{F}_{\varphi^2}(x)$. Then, combining (12), (17) and (21), (20) can be derived. □

*3.3. The Outage Probability of the OMA Benchmark.* For RIS-assisted non-terrestrial OMA networks, there is one time slot in the transmission of communications. Specifically, with the assistance of the RIS, the entire transmission process consists of the satellite sending the signals to two users in the same time slot. Hence the outage probability of the $p$-th user is defined to occur as the instantaneous SNR of the network, represented by $\gamma_p^{OMA}$, is less than a certain threshold in the slot while communicating. The outage probability of the RIS-assisted non-terrestrial NOMA networks via OMA benchmark can be expressed as

$$P_{D_p}^{OMA} = \Pr\left(\gamma_p^{OMA} < \gamma_{th}^{OMA}\right), \tag{23}$$

where $\gamma_{th}^{OMA} = 2^{R_p} - 1$ is the target SNR of the $p$-th user to detect and decode the signals.

**Theorem 4.** *Under large-scale fading and Nakagami-m fading cascaded channels, the approximate expression for outage probability of the p-th user for RIS-assisted non-terrestrial*

Table 1: The fixed numerical values of the parameters.

| Monte Carlo simulation repeated | $10^6$ iterations |
|---|---|
| Two users'power allocations | $a_n = 0.4$ |
| | $a_m = 0.6$ |
| Two users'target rates | $R_n = 0.05$BPCU |
| | $R_m = 0.04$BPCU |
| The lobe gains of Users'antennas | $G_i = 12$dB |
| The lobe gains of satellite's antennas | $G_t = 80$dB |
| Carrier frequency | $f_c = 3 \times 10^8$Hz |

*OMA networks is given by*

$$P_{D_p}^{OMA} \approx S_p \sum_{l=0}^{M-p} M - p_l \frac{(-1)^l}{(p+l)[\Gamma(a+1)]^{p+l}} \times \left[\gamma\left(a+1, \frac{\sqrt{\Theta_{oma}}}{\bar{\lambda}b}\right)\right]^{p+l}, \tag{24}$$

where $S_p = M!/(M-p)!(p-1)!$, $\Theta_{\text{oma}} = \gamma_{th}^{OMA}/\rho$

*3.4. Diversity Analysis.* For further evaluation of system performance, the diversity order is taken to be analysed. The diversity order is the limit value when the SNR tends to be infinity, and is particularly important to evaluate system performance under high SNR, because it is approximately the slope of the outage probability curve at high SNR regime. Thus, it can be used to assess the decreasing rate of the outage probability for communication systems. The diversity order can be expressed as

$$d = -\lim_{\rho \longrightarrow \infty} \frac{\log\left[P^{\infty}(\rho)\right]}{\log \rho}, \tag{25}$$

where $P^{\infty}(\rho)$ denotes the asymptotic outage probability.

**Corollary 5.** *The asymptotic outage probability expression of the nearby user n with ipSIC for RIS-assisted non-terrestrial NOMA networks when $\rho \longrightarrow \infty$ can be given by*

$$P_{D_n}^{\infty,ipSIC} = S_n \sum_{l=0}^{M-n} \sum_{u=0}^{U} M - n_l \frac{(-1)^l A_u}{(n+l)[\Gamma(a+1)]^{n+l}} \times \left[\gamma\left(a+1, \frac{\sqrt{\varpi \Omega_I \theta_n^{\rho} x_u}}{\bar{\lambda}b}\right)\right]^{n+l}, \tag{26}$$

where $\varpi = 1$, $\theta_n^{\rho} = \gamma_{th_n}/a_n$

*Remark 6.* Upon substituting (26) into (25), a zero diversity order for the nearby user n with ipSIC can be derived, this signifies that the outage probability curve eventually converges to a certain value in the high SNR regime. This phenomenon is due to the influence of the residual interference from ipSIC during the detecting and decoding process.

**Corollary 7.** *The asymptotic outage probability expression of the nearby user n with pSIC for RIS-assisted non-terrestrial NOMA networks when $\rho \longrightarrow \infty$ can be given by*

$$P_{D_n}^{\infty,pSIC} = \frac{S_n^{\infty} \theta^{n(a+1)/2}}{\left(\bar{\lambda}b\right)^{n(a+1)}[(a+1)\Gamma(a+1)]^n} \propto \frac{1}{\rho^{n(a+1)/2}}, \tag{27}$$

where $S_n^{\infty} = M!/(M-n)!n!$

*Proof.* According to the series representation of the lower incomplete gamma function ([44], Eq. (8.354.1)), the gamma function part of $P_{D_n}^{pSIC}$ can be further rewritten as

$$\gamma\left(a+1, \frac{\sqrt{\theta}}{\bar{\lambda}b}\right) = \sum_{n=0}^{\infty} \frac{(-1)^n \left(\sqrt{\theta}/\bar{\lambda}b\right)^{a+1+n}}{n!(a+1+n)}. \tag{28}$$

When $\rho \longrightarrow \infty$, $\theta \longrightarrow 0$. Then, by substituting (28) into (18), and further taking the first term of each series representation, i.e., $n = 0$ and $l = 0$, we can obtain (27). The proof is completed. □

*Remark 8.* Upon substituting (27) into (25), the diversity order of the nearby user n with pSIC is equal to $nK[E(\varphi_n)]^2/2Var(\varphi_n)$, which is related to the order of the nearby user, and Nakagami-m parameter m′ and Ω

**Corollary 9.** *The asymptotic outage probability expression of the distant user m for RIS-assisted non-terrestrial NOMA network when $\rho \longrightarrow \infty$ can be given by*

$$P_{D_m}^{\infty} = \frac{S_m^{\infty} \gamma^{* m(a+1)/2}}{\left(\bar{\lambda}b\right)^{m(a+1)}[(a+1)\Gamma(a+1)]^m} \propto \frac{1}{\rho^{m(a+1)/2}}, \tag{29}$$

where $S_m^{\infty} = M!/(M-m)!m!$

*Remark 10.* By substituting (29) into (25), it can be derived that the diversity order of the distant user m is equal to $mK[E(\varphi_n)]^2/2Var(\varphi_n)$, which is also related to the order of the distant user, and Nakagami-m parameter $m'$ and Ω

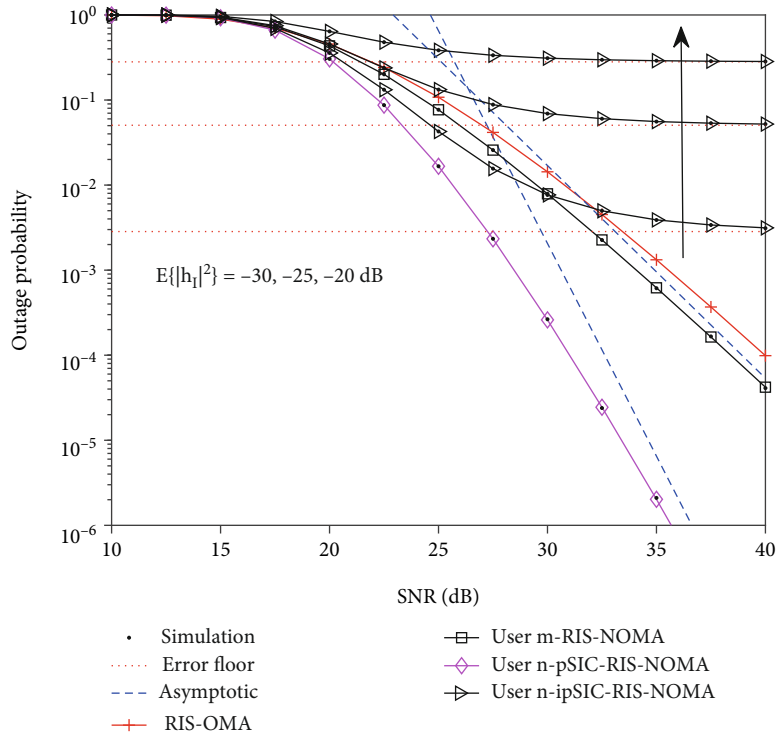


Figure 2: Outage probability versus the transmit SNR, with $K = 5$, $m' = 0.5$, $d = 300$ km, $\Omega = 1$, $R_n = 0.05$ and $R_m = 0.04$ BPCU

## 4. Simulation and Numerical Results

In this section, simulation analysis of the outage probability for RIS-assisted non-terrestrial NOMA networks is provided to adequately confirm the previous conclusions form the above subsections. Listing statistics for convenience, Table 1 shows the fixed numerical values of the parameters used in this paper [9, 39, 43] and BPCU is the abbreviation of bit per channel use. Without loss of generality, the method of controlling variables is adopted, we just change only a certain parameter to analyze the probability of outage in this scenario for a more intuitive expression. To make the scenario more specific to evaluate performance, in the simulations, the total number of users $M$ is set as three, the $n$-th user is set as the first user and the $m$-th user is set as the second user (It is set that $M = 3, m = 2, n = 1$). In addition, RIS-assisted non-terrestrial OMA is also select to be included in the analysis as a benchmark for comparison. It is worth pointing that the detecting target rate for OMA benchmark of the entire networks is set to be $R_m + R_n$

Figure 2 illustrates the outage probability of the RIS-assisted non-terrestrial NOMA networks versus the transmit SNR with settings of $K = 5$, $m' = 0.5$, $d = 300$ km, $\Omega = 1$, $R_n = 0.05$ and $R_m = 0.04$ BPCU, and compares the condition of different value of residual interference for ipSIC scheme at the same time. As shown in the figure, according to (14) and (18), the expression of the outage probability for user $n$ with ipSIC/pSIC can be plotted as the right triangle and diamond solid curves, respectively. According to (20), the exact expression of the outage probability for user $m$ can be plotted as the square solid curve, and the cross curve for outage probability of the RIS-assisted non-terrestrial OMA is plotted based on (24). The outage probability curve obtained from the numerical simulation results fits perfectly with the curve drawn by the formula derived from the above subsections. It can be observed that for the nearby user $n$, the outage performance is better in the pSIC scheme than ipSIC scheme because of the existence of residual interference, and when the residual interference gradually decreases, under a certain range of SNR, the curves gradually fit. For the comparison between RIS-assisted non-terrestrial NOMA and OMA, it can be proofed that NOMA scheme performs better than OMA scheme, it is because that in NOMA scheme, multiple users receive the spectrum resource with power allocation to bring about better fairness relative to OMA [7], and SIC process at the receive-end can also help to increase the received SINR. According to (26), (27) and (29), the exact expression of the asymptotic outage probability for user $n$ with pSIC and user $m$ can be plotted as the blue dotted curve and that of the user $n$ with ipSIC can be plotted as the red dotted curve, respectively. The asymptotic curves can well represent the performance of the networks under high SNR, so that the results can be displayed more intuitively. It can be observed that through the comparison between the asymptotic outage probability of uesr $n$ with pSIC and uesr $m$, the former performs better than the latter. Confirmed by Remark 6, the outage probability of uesr $n$ with ipSIC eventually gets a zero diversity order and converges to an error floor because of the impact of the residual interference. Hence, the outage performance of the nearby user $n$ with ipSIC is worse than that of other

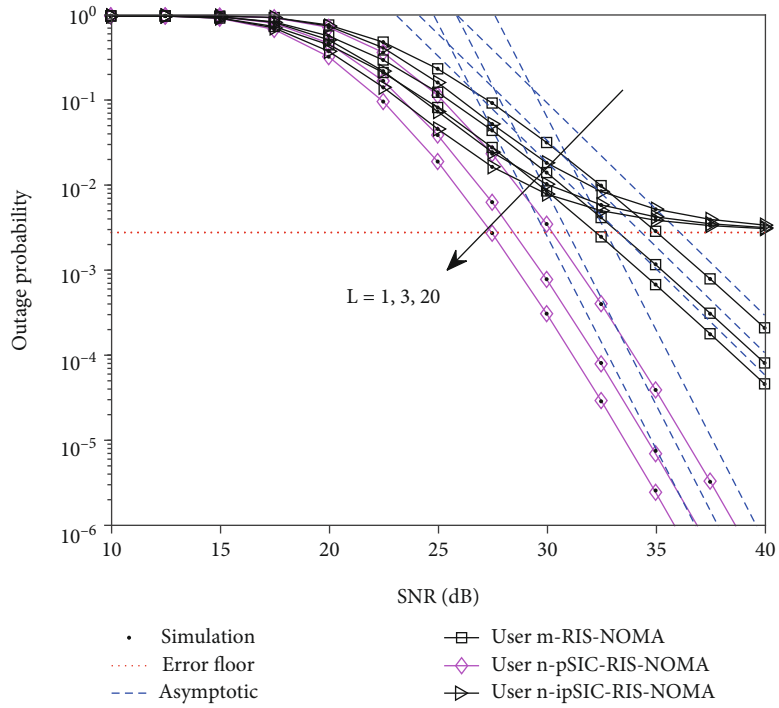


FIGURE 3: Outage probability versus the transmit SNR for various length of training symbols, with $K = 5$, $m' = 0.5$, $d = 300$ km, $\Omega = 1$, $E\{|h_I|^2\} = -30$ dB, $R_n = 0.05$ and $R_m = 0.04$ BPCU

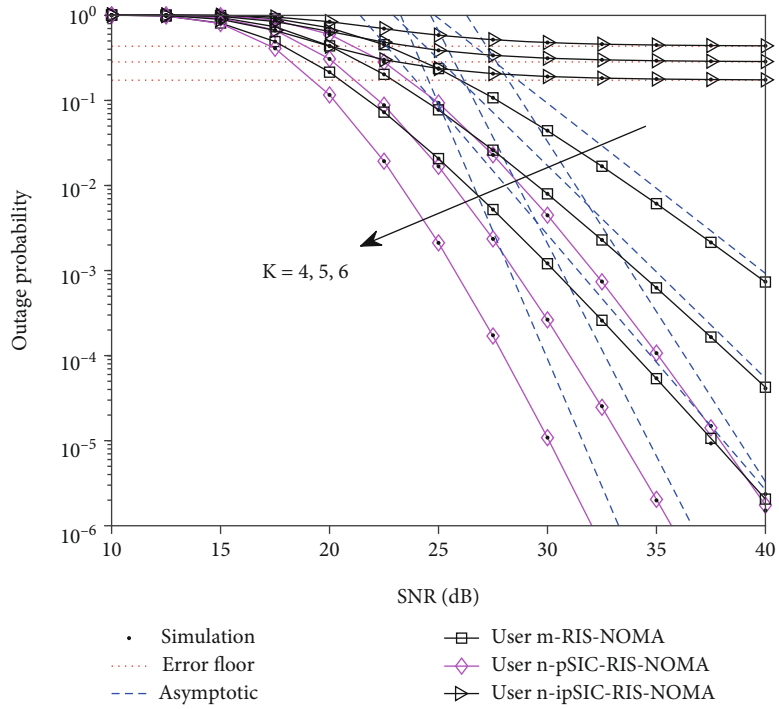


FIGURE 4: Outage probability versus the transmit SNR, with $m' = 0.5$, $d = 300$ km, $\Omega = 1$, $E\{|h_I|^2\} = -20$ dB, $R_n = 0.05$ and $R_m = 0.04$ BPCU

users'conditions, and it is kind crucial to take the residual interference into consideration when it comes to a practical communication scenario.

Under actual channel environment conditions, it is not easy to estimate channel state information (CSI) between the satellite and terrestrial nodes, so we also consider the imperfect

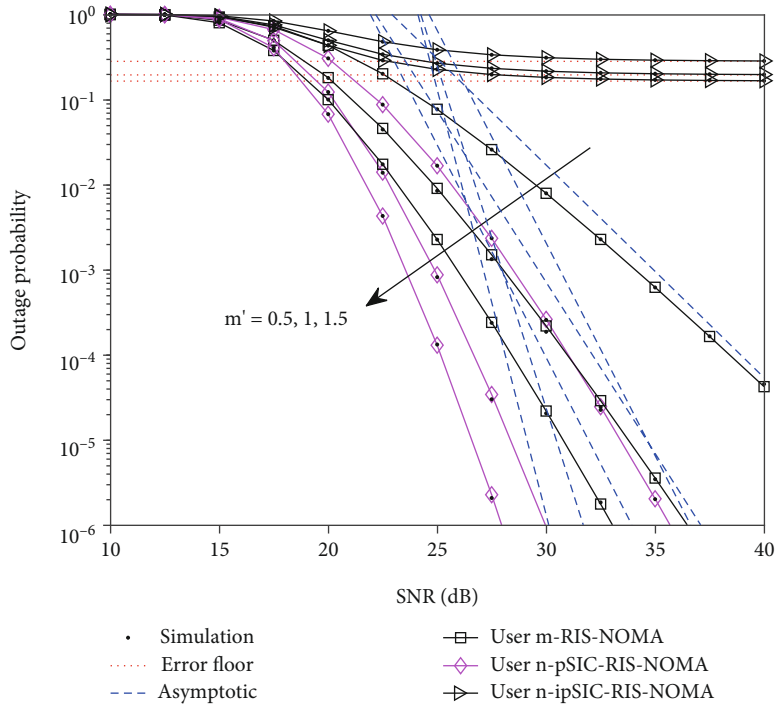


FIGURE 5: Outage probability versus the transmit SNR, with $K = 5$, $d = 300$ km, $\Omega = 1$, $E\{|h_I|^2\} = -20$ dB, $R_n = 0.05$ and $R_m = 0.04$ BPCU

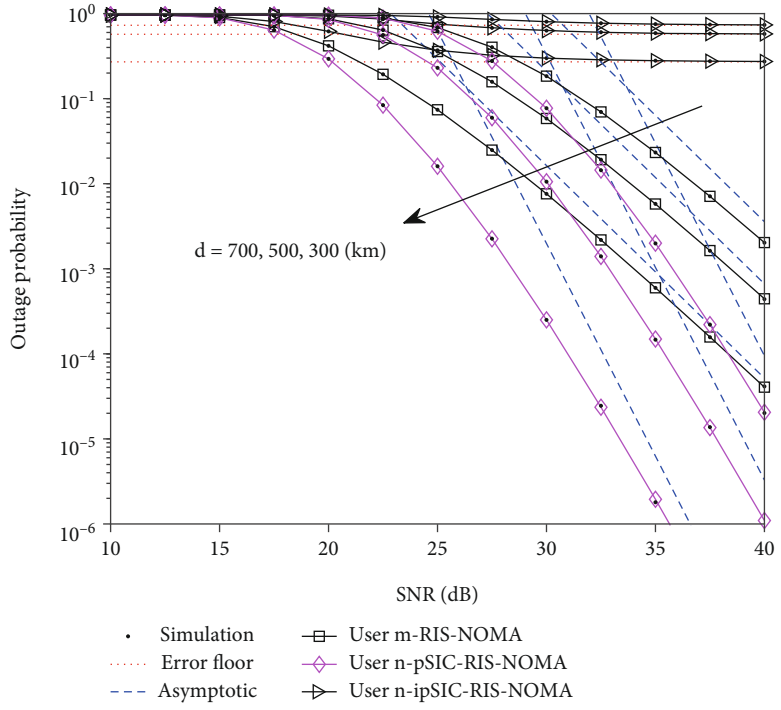


FIGURE 6: Outage probability versus the transmit SNR, with $K = 5$, $m' = 0.5$, $\Omega = 1$, $E\{|h_I|^2\} = -20$ dB, $R_n = 0.05$ and $R_m = 0.04$ BPCU

CSI scenario. The receiver uses the minimum mean square error to estimate the channel coefficients, which can be modeled as $h\bar{\Theta}\mathbf{g}_p^T = h\Theta\mathbf{g}_p^T + e_k$, where $e_k$ denote the estimated channel error with $e_k \sim CN(0, \sigma_{ek}^2)$. $L$ represents the lengths of training symbols for CSI estimation and the variance of estimated channel error can be denoted by $\sigma_{ek}^2 = 1/\rho L$. Figure 3 illustrates the outage probability of the RIS-assisted non-terrestrial NOMA networks versus the transmit SNR with settings of $K = 5$, $m' = 0.5$, $d = 300$ km, $\Omega = 1$, $E\{|h_I|^2\} = -30$ dB, $R_n = 0.05$ and $R_m = 0.04$ BPCU, and compares the

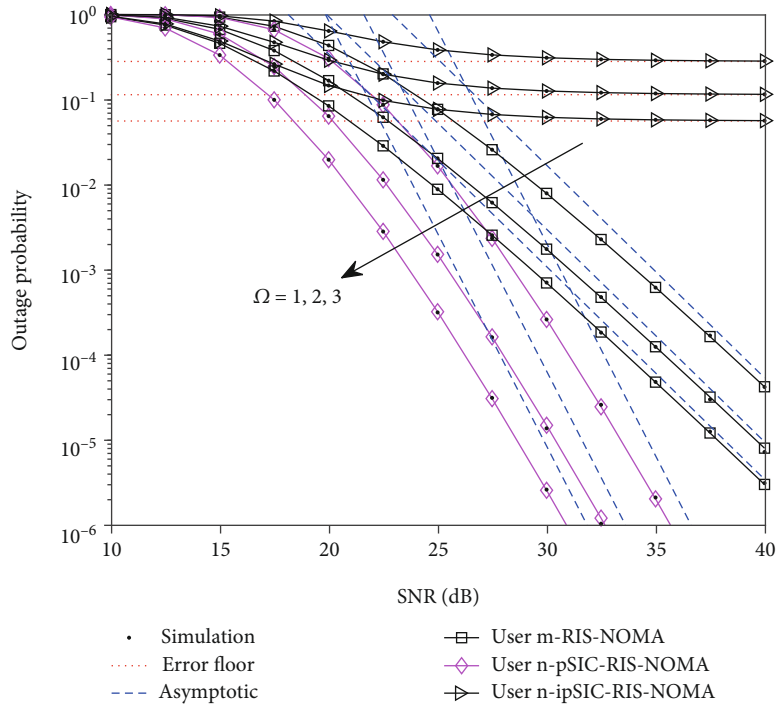


FIGURE 7: Outage probability versus the transmit SNR, with $K = 5$, $d = 300$ km, $m' = 0.5$, $E\{|h_I|^2\} = -20$ dB, $R_n = 0.05$ and $R_m = 0.04$ BPCU

condition of different value of training times at the same time. The situation becomes ideal CSI as $L$ approaches infinity. Under high SNR, the outage probability of nearby user with ipSIC scheme tends to be consistent with different training amounts due to the impact of the residual interference. It can be observed from the simulation that with the increase of $L$, the improvement of outage performance tends to be slow. Therefore in practical applications, we can also increase the lengths of the training symbols to approach better performance.

The impact of the number of reflecting elements on RIS $K$ for the performance of the networks is significant, and it is shown in Figure 4, which plots the outage probability of the RIS-assisted non-terrestrial NOMA networks versus the transmit SNR with settings of $m' = 0.5$, $d = 300$ km, $\Omega = 1$, $E\{|h_I|^2\} = -20$ dB, $R_n = 0.05$ and $R_m = 0.04$ BPCU, and compares the condition of different number of reflecting elements on RIS, $K$, at the same time. It can be seen intuitively from the figure, the outage performance is significantly affected by the number of reflecting elements on RIS for a specification of more reflecting elements, smaller outage probability of user $n$ and user $m$ in the RIS-assisted non-terrestrial NOMA networks. Meanwhile, in line with Remark 8 and Remark 10, it can be observed that diversity orders of non-orthogonal users are affected by the reflecting elements on RIS, $K$. When $K$ grows, the slope of the diversity orders for both user $n$ and user $m$ increase. It is worth mentioning that when it comes to the sorted channel, the diversity order will be related to the ordinal number of the current user. Therefore, in practical applications, we can change the value of K according to the change of the actual channel environment in order to achieve a better communication effect. Figure 5 illustrates the outage probability of the RIS-assisted non-terrestrial NOMA networks versus the transmit SNR with settings of $K = 5$, $d = 300$ km, $\Omega = 1$, $E\{|h_I|^2\} = -20$ dB, $R_n = 0.05$ and $R_m = 0.04$ BPCU, and compares the condition of different value of Nakagami-$m$ shaping parameter $m'$ at the same time. As we can see form the figure, outage performance gradually gets better as Nakagami-$m$ shaping parameter $m'$ increases. For Nakagami-$m$ distribution, Nakagami-$m$ shaping parameter $m'$ represents the fading environment, when $m'$ grows, the fading environment gets better, when $m$ approaches infinity, it means no fading. Hence it is needed to carefully consider the shaping parameter $m'$ of the environmental channel when we apply it to the actual scene.

Figure 6 illustrates the outage probability of the RIS-assisted non-terrestrial NOMA networks versus the transmit SNR with settings of $K = 5$, $m' = 0.5$, $\Omega = 1$, $E\{|h_I|^2\} = -20$ dB, $R_n = 0.05$ and $R_m = 0.04$ BPCU, and compares the condition of different value of distance from satellite to ground at the same time. The distance from satellite to ground determines the path loss factor in large-scale fading scenarios, when the distance increases, the path loss factor increases. Therefore, it can be clearly seen from the figure that when the distance decreases, the outage performance of the non-orthogonal users gradually improves. However, because the distance to the ground of the satellite is standardized, it should be considered according to practical scenarios. Taking consideration of another factor for Nakagami-$m$ fading, Figure 7 illustrates the outage

probability of the RIS-assisted non-terrestrial NOMA networks versus the transmit SNR with settings of $K = 5$, $d = 300$ km, $m' = 0.5$, $E\{|h_I|^2\} = -20$ dB, $R_n = 0.05$ and $R_m = 0.04$ BPCU, and compares the condition of different value of scale parameter of Nakagami-$m$ fading $\Omega$ at the same time. The actual meaning of $\Omega$ is the fading power of Nakagami-$m$ fading, its physical meaning is the mean of the square of the signal envelope, when the value of $\Omega$ increases, the channel condition will become better, and the outage performance of the users become better.

## 5. Conclusion

In this paper, a RIS-assisted non-terrestrial NOMA networks with large-scale fading and Nakagami-$m$ fading cascaded channels has been discussed in detail. More specifically, the approximate expression for outage probability of nearby user $n$ with ipSIC/pSIC and distant user $m$, and asymptotic expression for outage probability of user $n$ with pSIC and user $m$ under the sorted user channel schemes have been derived carefully. Based on the analysis of the outage performance, the diversity order is also obtained to evaluate the outage performance. Meanwhile, the influence of each variable to the system performance is analysed. Eventually, through detailed study of this paper, we can find that the performance of RIS-assisted non-terrestrial NOMA is better than that of OMA, and the cascaded channel scenario can obtain a more ideal transmission effect through the propagation of RIS and the optimization of parameters in the future studying.

## Data Availability

The calculation and simulation data used to support the findings of this study are included within the article.

## Conflicts of Interest

The author(s) declare(s) that they have no conflicts of interest.

## Acknowledgments

This work was supported by the National Natural Science Foundation of China under grant 62071052 and grant 62201533 and the R&D Program of Beijing Municipal Education Commission under grant KM202011232003.

## References

[1] Y. Ji, J. Zhang, Y. Xiao, and Z. Liu, "5G flexible optical transport networks with large-capacity, low-latency and high-efficiency," *China Communications*, vol. 16, no. 5, pp. 19–32, 2019.

[2] X. You, C. X. Wang, J. Huang et al., "Towards 6G wireless communication networks: Vision, enabling technologies, and new paradigm shifts," *Science China Information Sciences*, vol. 64, no. 1, 2021.

[3] Y. Liu, Z. Qin, M. Elkashlan, Z. Ding, A. Nallanathan, and L. Hanzo, "Nonorthogonal multiple access for 5G and beyond," *Proceedings of the IEEE*, vol. 105, no. 12, pp. 2347–2381, 2017.

[4] X. Liu, B. Lin, M. Zhou, and M. Jia, "NOMA-Based cognitive spectrum access for 5G-enabled internet of things," *IEEE Network*, vol. 35, no. 5, pp. 290–297, 2021.

[5] X. Pei, Y. Chen, M. Wen, H. Yu, E. Panayirci, and H. V. Poor, "Next-Generation multiple access based on NOMA with power level modulation," *IEEE Journal on Selected Areas in Communications*, vol. 40, no. 4, pp. 1072–1083, 2022.

[6] Z. Ding, Z. Yang, P. Fan, and H. V. Poor, "On the performance of non-orthogonal multiple access in 5G systems with randomly deployed users," *IEEE Signal Processing Letters*, vol. 21, no. 12, pp. 1501–1505, 2014.

[7] Z. Ding, Y. Liu, J. Choi et al., "Application of non-orthogonal multiple access in LTE and 5G networks," *IEEE Communications Magazine*, vol. 55, no. 2, pp. 185–191, 2017.

[8] X. Yue, Z. Qin, Y. Liu, S. Kang, and Y. Chen, "A unified framework for non-orthogonal multiple access," *IEEE Transactions on Communications*, vol. 66, no. 11, pp. 5346–5359, 2018.

[9] X. Yue, Y. Liu, S. Kang, A. Nallanathan, and Z. Ding, "Exploiting full/half-duplex user relaying in NOMA systems," *IEEE Transactions on Communications*, vol. 66, no. 2, pp. 560–575, 2018.

[10] D. Wan, M. Wen, F. Ji, Y. Liu, and Y. Huang, "Cooperative NOMA systems with partial channel state information over nakagami- $m$ fading channels," *IEEE Transactions on Communications*, vol. 66, no. 3, pp. 947–958, 2018.

[11] Y. Liu, Z. Qin, M. Elkashlan, Y. Gao, and L. Hanzo, "Enhancing the physical layer security of non-orthogonal multiple access in large-scale networks," *IEEE Transactions on Wireless Communications*, vol. 16, no. 3, pp. 1656–1672, 2017.

[12] W. Chen, H. Ding, S. Wang, D. B. da Costa, F. Gong, and P. H. Juliano Nardelli, "Backscatter cooperation in NOMA communications systems," *IEEE Transactions on Wireless Communications*, vol. 20, no. 6, pp. 3458–3474, 2021.

[13] Z. Ding, R. Schober, P. Fan, and H. V. Poor, "Simple Semi-Grant-Free transmission strategies assisted by non-orthogonal multiple access," *IEEE Transactions on Communications*, vol. 67, no. 6, pp. 4464–4478, 2019.

[14] R. Huang, D. Wan, F. Ji et al., "Performance analysis of NOMA-based cooperative networks with relay selection," *China Communications*, vol. 17, no. 11, pp. 111–119, 2020.

[15] D. Wan, R. Huang, M. Wen, G. Chen, F. Ji, and J. Li, "A simple multicarrier transmission technique combining transmit diversity and data multiplexing for non-orthogonal multiple access," *IEEE Transactions on Vehicular Technology*, vol. 70, no. 7, pp. 7216–7220, 2021.

[16] G. Araniti, A. Iera, S. Pizzi, and F. Rinaldi, "Toward 6G non-terrestrial networks," *IEEE Network*, vol. 36, no. 1, pp. 113–120, 2022.

[17] S. Chen, S. Sun, and S. Kang, "System integration of terrestrial mobile communication and satellite communication —the trends, challenges and key technologies in B5G and 6G," *China Communications*, vol. 17, no. 12, pp. 156–171, 2020.

[18] V. Singh and P. K. Upadhyay, "Exploiting FD/HD cooperative-NOMA in underlay cognitive hybrid satellite-terrestrial networks," *IEEE Transactions on Cognitive Communications and Networking*, vol. 8, no. 1, pp. 246–262, 2022.

[19] N. Wang, F. Li, D. Chen, L. Liu, and Z. Bao, "NOMA-based Energy-Efficiency optimization for UAV enabled space-air-ground integrated relay networks," *IEEE Transactions on Vehicular Technology*, vol. 71, no. 4, pp. 4129–4141, 2022.

[20] A. A. Nasir, H. D. Tuan, T. Q. Duong, and H. V. Poor, "UAV-Enabled communication using NOMA," *IEEE Transactions on Communications*, vol. 67, no. 7, pp. 5126–5138, 2019.

[21] R. Ge, D. Bian, J. Cheng, K. An, J. Hu, and G. Li, "Joint user Pairing and power allocation for NOMA-based GEO and LEO satellite network," *IEEE Access*, vol. 9, pp. 93255–93266, 2021.

[22] Z. Gao, A. Liu, and X. Liang, "The performance analysis of downlink NOMA in LEO satellite communication system," *IEEE Access*, vol. 8, pp. 93723–93732, 2020.

[23] X. Yue, Y. Liu, Y. Yao et al., "Outage behaviors of NOMA-based satellite network over Shadowed-Rician fading channels," *IEEE Transactions on Vehicular Technology*, vol. 69, no. 6, pp. 6818–6821, 2020.

[24] X. Zhang, B. Zhang, K. An et al., "Outage performance of NOMA-based cognitive hybrid satellite-terrestrial overlay networks by amplify-and-forward protocols," *IEEE Access*, vol. 7, pp. 85372–85381, 2019.

[25] L. Han, W.-P. Zhu, and M. Lin, "Outage of NOMA-based hybrid satellite-terrestrial multi-antenna DF relay networks," *IEEE Wireless Communications Letters*, vol. 10, no. 5, pp. 1083–1087, 2021.

[26] Y. Liu, X. Liu, X. Mu et al., "Reconfigurable intelligent surfaces: Principles and opportunities," *IEEE Communication Surveys and Tutorials*, vol. 23, no. 3, pp. 1546–1577, 2021.

[27] S. Lin, B. Zheng, G. C. Alexandropoulos, M. Wen, M. D. Renzo, and F. Chen, "Reconfigurable intelligent surfaces with reflection pattern modulation: beamforming design and performance analysis," *IEEE Transactions on Wireless Communications*, vol. 20, no. 2, pp. 741–754, 2021.

[28] S. Basharat, S. A. Hassan, H. Pervaiz, A. Mahmood, Z. Ding, and M. Gidlund, "Reconfigurable intelligent surfaces: potentials, applications, and challenges for 6G wireless networks," *IEEE Wireless Communications*, vol. 28, no. 6, pp. 184–191, 2021.

[29] A.-A. A. Boulogeorgos and A. Alexiou, "Performance analysis of reconfigurable intelligent surface-assisted wireless systems and comparison with relaying," *IEEE Access*, vol. 8, pp. 94463–94483, 2020.

[30] C. Zhang, W. Yi, Y. Liu, K. Yang, and Z. Ding, "Reconfigurable Intelligent surfaces aided multi-cell NOMA networks: a stochastic geometry model," *IEEE Transactions on Communications*, vol. 70, no. 2, pp. 951–966, 2022.

[31] Y. Cheng, K. H. Li, Y. Liu, K. C. Teh, and G. K. Karagiannidis, "Nonorthogonal multiple access (NOMA) with multiple intelligent reflecting surfaces," *IEEE Transactions on Communications*, vol. 20, no. 11, pp. 7184–7195, 2021.

[32] X. Yue and Y. Liu, "Performance analysis of intelligent reflecting surface assisted NOMA networks," *IEEE Transactions on Wireless Communications*, vol. 21, no. 4, pp. 2623–2636, 2022.

[33] Z. Ding and H. Vincent Poor, "A simple design of IRS-NOMA transmission," *IEEE Communications Letters*, vol. 24, no. 5, pp. 1119–1123, 2020.

[34] X. Mu, Y. Liu, L. Guo, J. Lin, and R. Schober, "Simultaneously transmitting and reflecting (STAR) RIS aided wireless communications," *IEEE Transactions on Wireless Communications*, vol. 21, no. 5, pp. 3083–3098, 2022.

[35] X. Zhou, K. Ying, S. Liu, M. Ke, Z. Gao, and M.-S. Alouini, "Reconfigurable intelligent surface assisted grant-free massive access," *Intell and Converged Network*, vol. 3, no. 1, pp. 134–143, 2022.

[36] R. Long, Y.-C. Liang, Y. Pei, and E. G. Larsson, "Active reconfigurable intelligent surface-aided wireless communications," *IEEE Transactions on Wireless Communications*, vol. 20, no. 8, pp. 4962–4975, 2021.

[37] N. Bhargav, C. R. N. da Silva, Y. J. Chun, E. J. Leonardo, S. L. Cotton, and M. D. Yacoub, "On the product of two <inline-formula> <tex-math notation="LaTeX">$\kappa$ </tex-math></inline-formula>–<inline-formula> <tex-math notation="LaTeX">$\mu$ </tex-math></inline-formula> random variables and its application to double and composite fading channels," *IEEE Transactions on Wireless Communications*, vol. 17, no. 4, pp. 2457–2470, 2018.

[38] Z. Ding, R. Schober, and H. V. Poor, "On the impact of phase shifting designs on IRS-NOMA," *IEEE Wireless Communications Letters*, vol. 9, no. 10, pp. 1596–1600, 2020.

[39] T. Li, X. Hao, and X. Yue, "A power domain multiplexing based cocarrier transmission method in hybrid satellite communication networks," *IEEE Access*, vol. 8, pp. 120036–120043, 2020.

[40] X. Yue, J. Xie, Y. Liu, Z. Han, R. Liu, and Z. Ding, "Simultaneously Transmitting and Reflecting Reconfigurable Intelligent Surface Assisted NOMA Networks,," (2021), https://arxiv.org/abs/2112.01336.

[41] H. Wang, Z. Shi, Y. Fu, and S. Fu, "On intelligent reflecting Surface-Assisted NOMA uplinks with imperfect SIC," *IEEE Wireless Communications Letters*, vol. 11, no. 7, pp. 1518–1522, 2022.

[42] Y. S. Cho, J. Kim, W. Y. Yang, and C. G. Kang, *MIMO-OFDM Wireless Communications with MATLAB*, Publishing House of Electronics Industry, Beijing, China, 2013.

[43] M. D. Yacoub, "The $\kappa$-$\mu$ distribution and the $\eta$-$\mu$ distribution," *IEEE Antennas and Propagation Magazine*, vol. 49, no. 1, pp. 68–81, 2007.

[44] I. S. Gradshteyn and I. M. Ryzhik, *Table of Integrals, Series and Products*, Academic Press, New York, NY, USA, 6th edition, 2000.

[45] V. Primak and V. Lyandres, *Stochastic Methods and their Applications to Communications: Stochastic Differential Equations Approach*, Wiley, West Sussex, U.K., 2004.

[46] H. A. David and H. N. Nagaraja, *Order Statistics*, Wiley, Hoboken, NJ, USA, 3rd edition, 2003.